

Supplementary Information

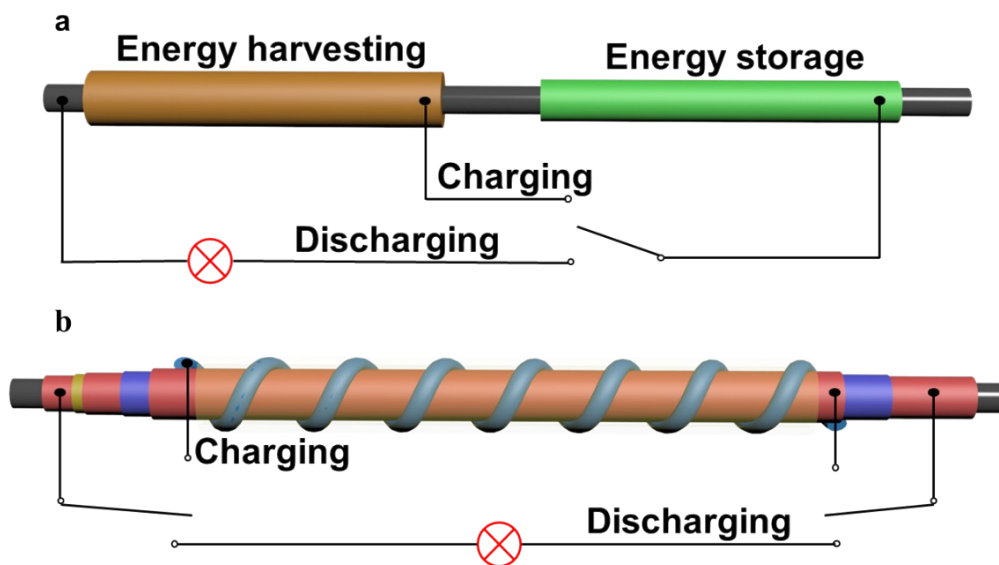


Figure S1. Schematic illustration to the two typical architectures of the self-powering fiber. (a) Fabrication of the energy harvesting and storing parts in series. (b) Coaxial fabrication of the energy harvesting and storing parts.

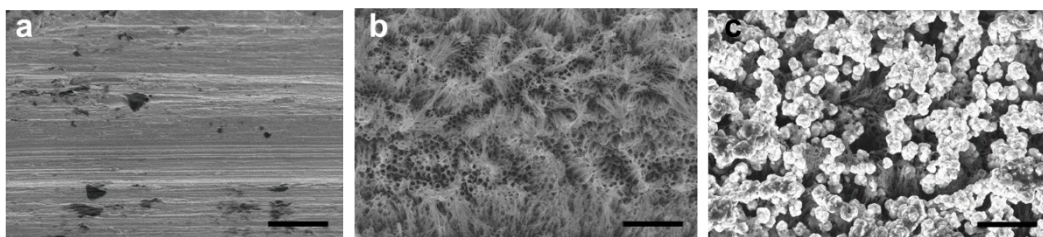


Figure S2. SEM images of modified photoanode fiber. (a) Titanium wire. (b) Aligned titania nanotubes. (c) CuI particle layer. Scale bar, 1 μm .

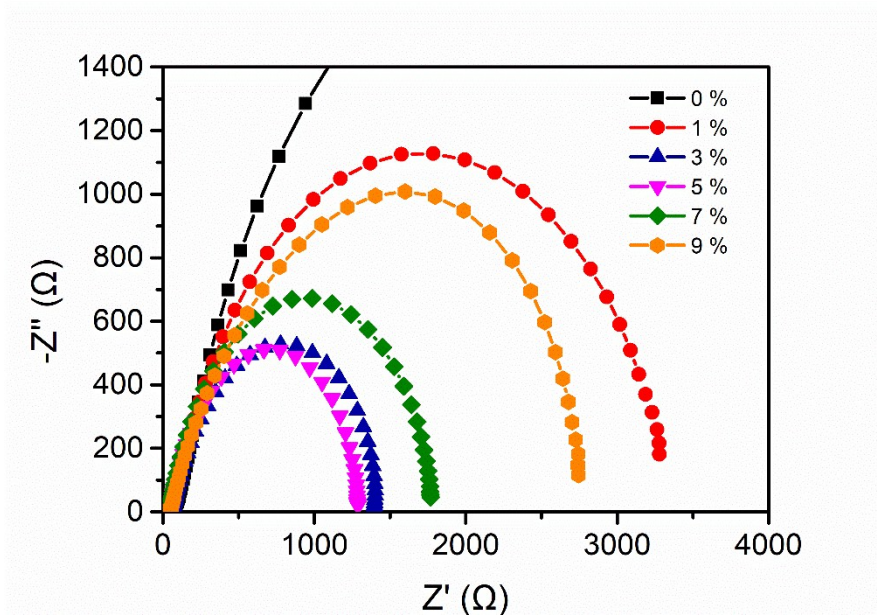


Figure S3. Nyquist plots of the PC part when the EMISCN concentrations were changed (inset, an equivalent circuit used to fit Nyquist plots).

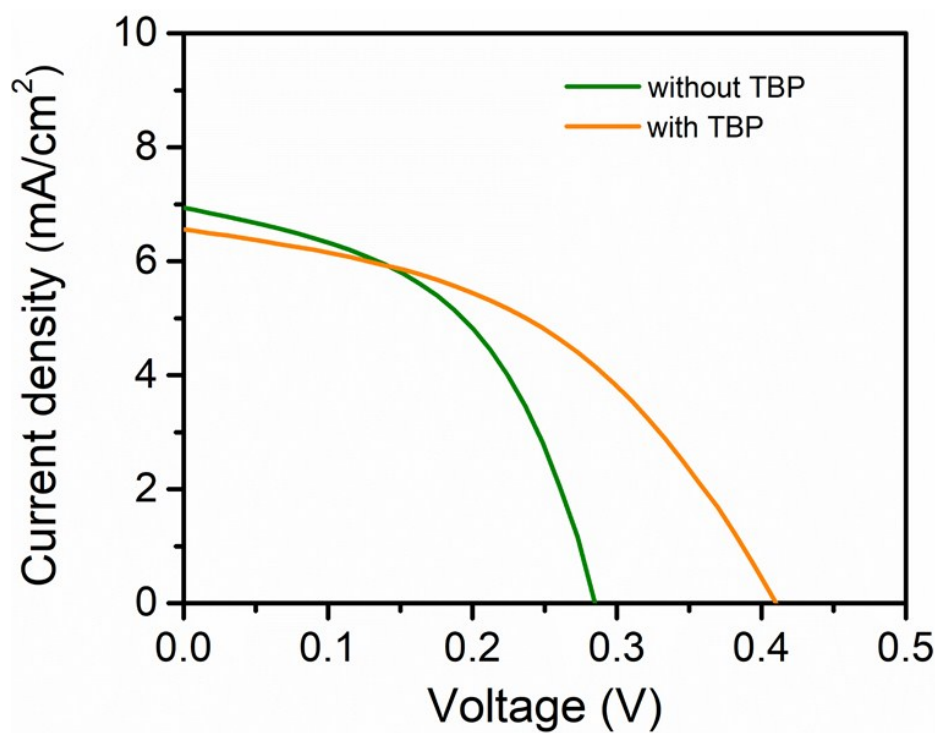


Figure S4. Photovoltaic performance of the PC part with and without addition of TBP.

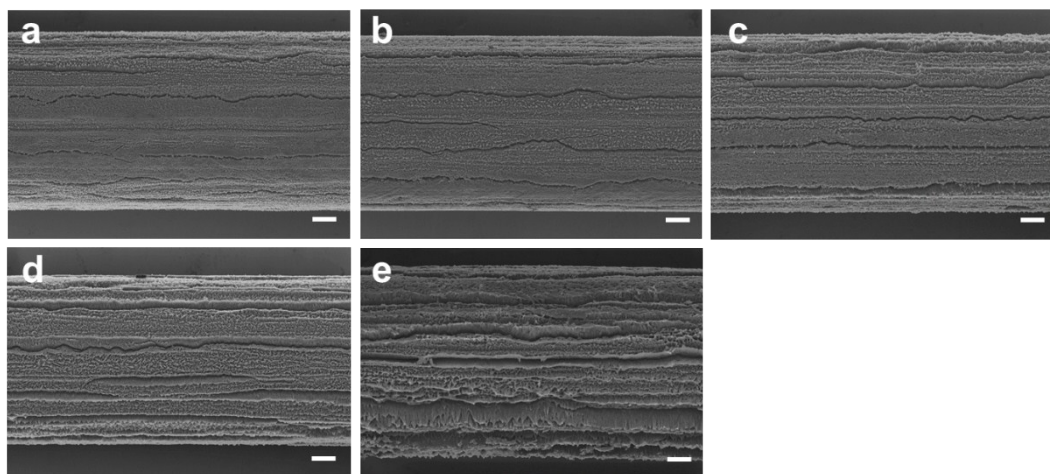


Figure S5. (a-e) SEM images of aligned titania nanotubes derived from anodic oxidation time of 1, 1.5, 2, 2.5, and 3 h, respectively. Scale bar, 20 μm .

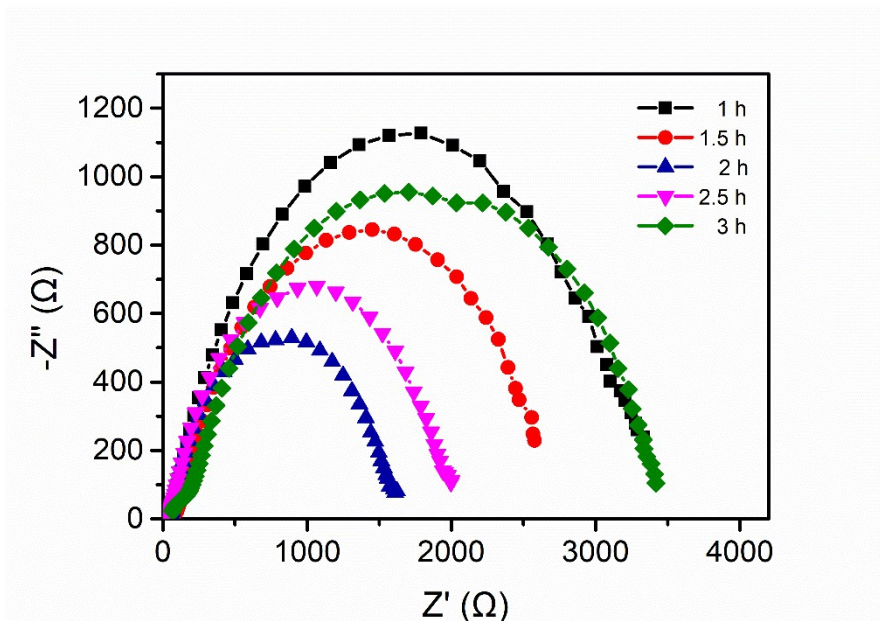


Figure S6. Nyquist plots of the PC part when the EMISCN concentration and anodic oxidation time were changed (inset, an equivalent circuit used to fit Nyquist plots).

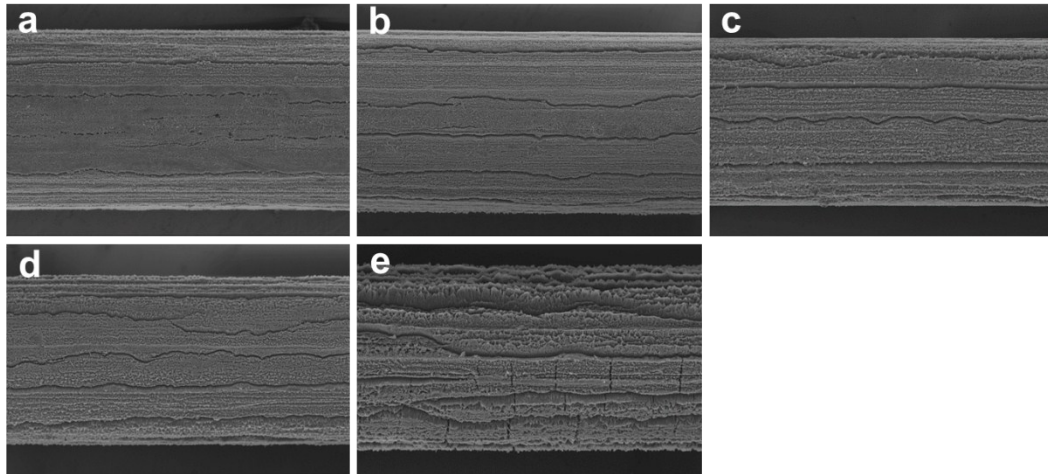


Figure S7. (a-e) SEM images of aligned titania nanotubes derived from anodic oxidation temperatures of 30°C, 35°C, 40°C, 45 °C, and 50 °C, respectively. Scale bar, 20 μm .

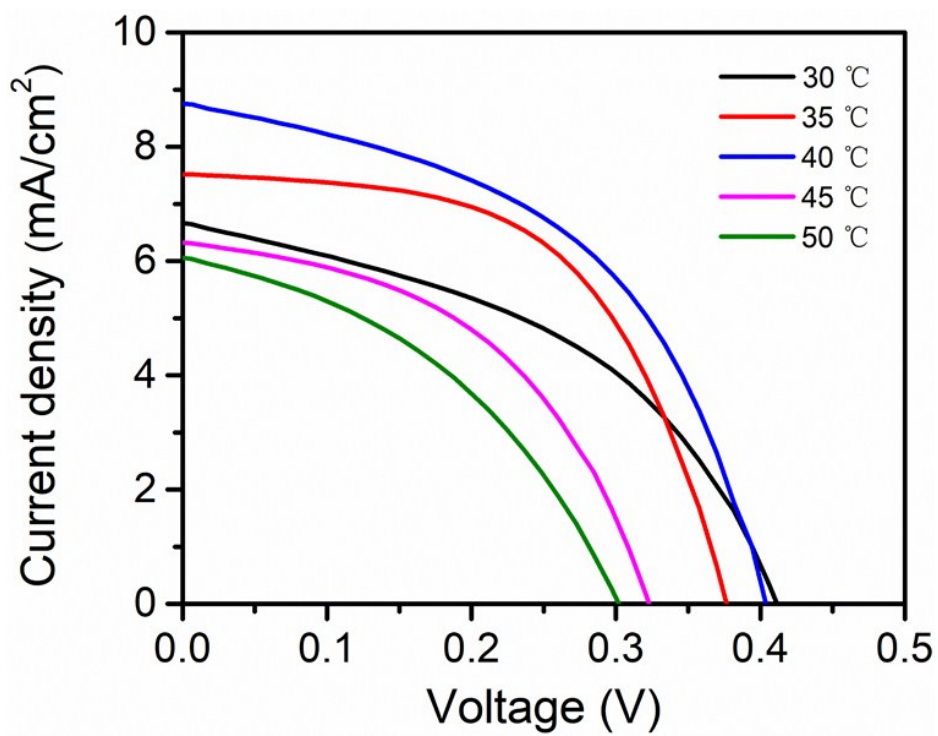


Figure S8. Photovoltaic performance of the PC part derived from different anodic oxidation temperatures.

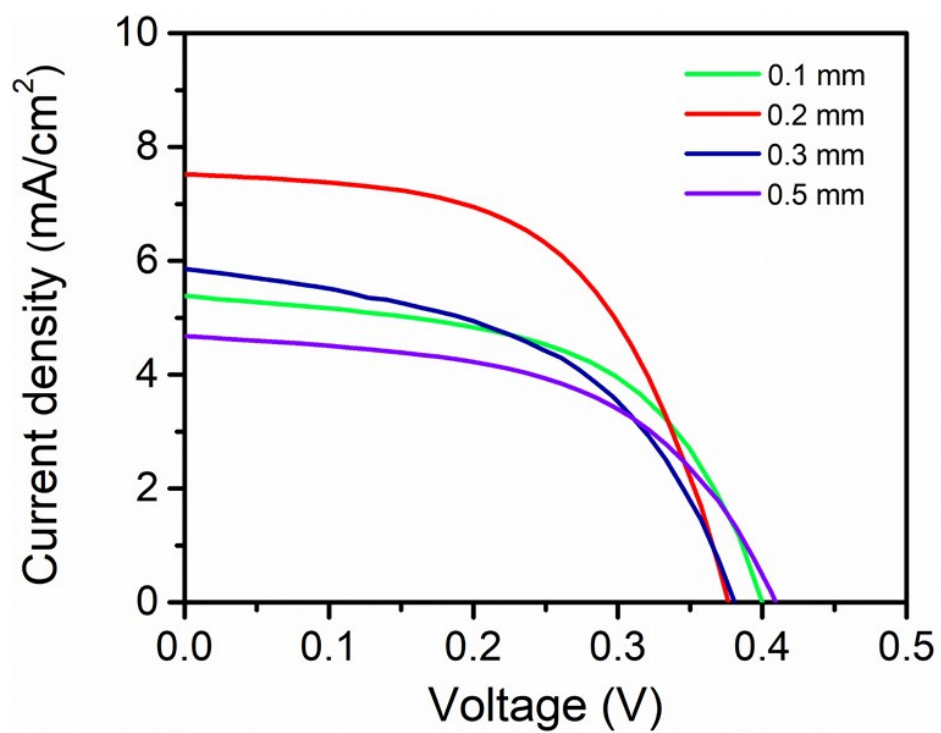


Figure S9. Dependence of the photovoltaic performance of the PC part on the diameter of the Ag-plated nylon yarn.

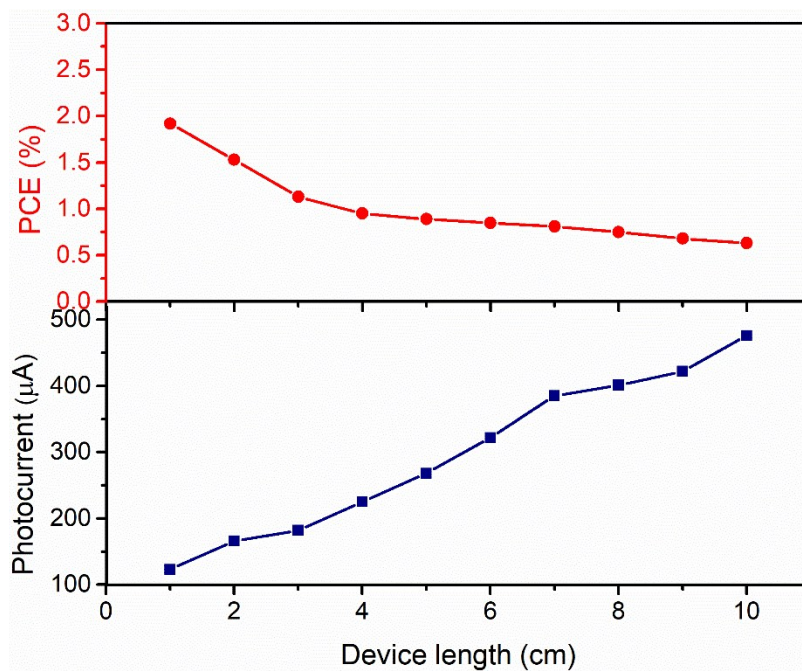


Figure S10. Photovoltaic performances of the PC part with increasing lengths.

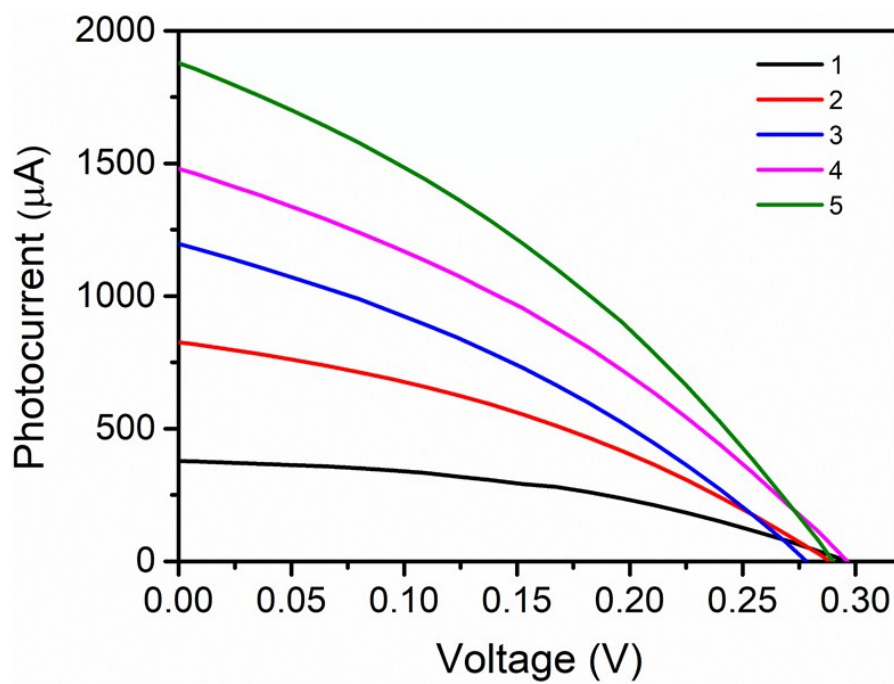


Figure S11. Current-voltage curves of the PC part with increasing numbers of modified photoanode fibers connected in parallel.

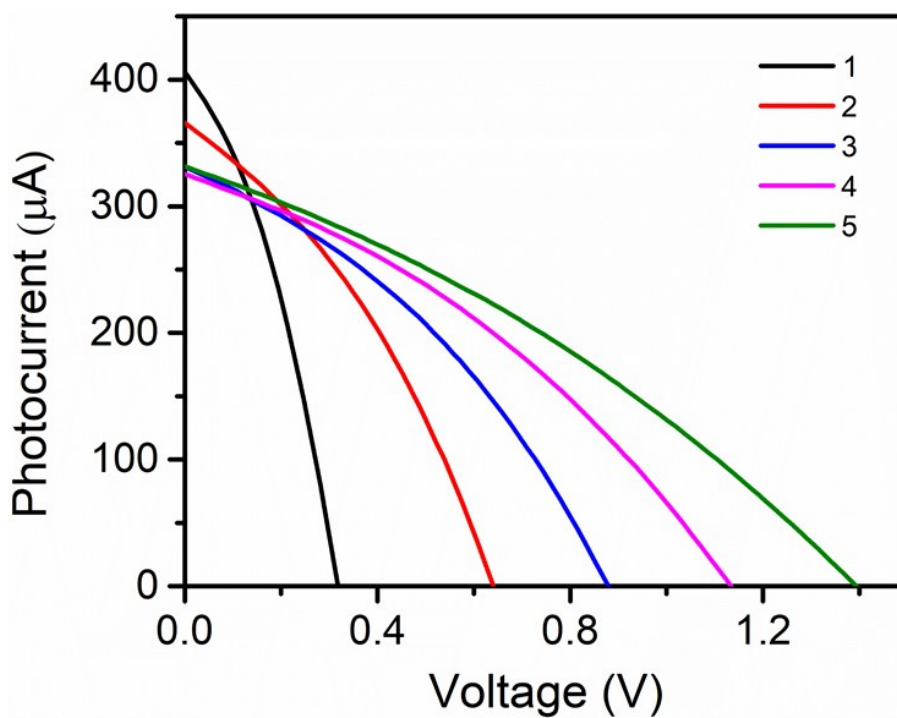


Figure S12. Current-voltage curves of the PC part with increasing numbers of modified photoanode fibers connected in series.

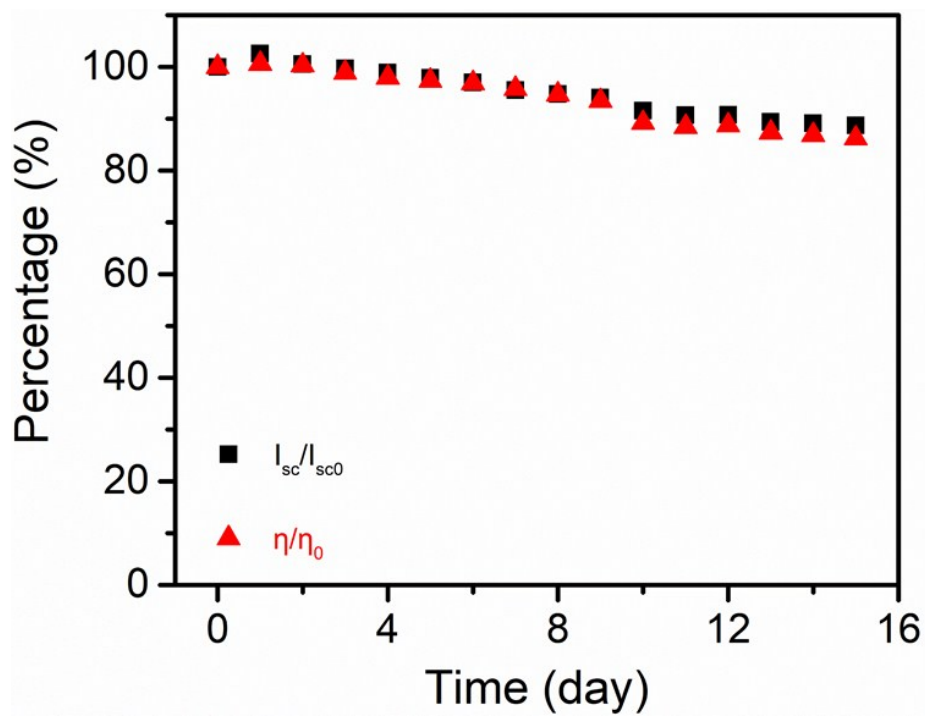


Figure S13. Dependence of photocurrent and PCE on time for the PC part in air.

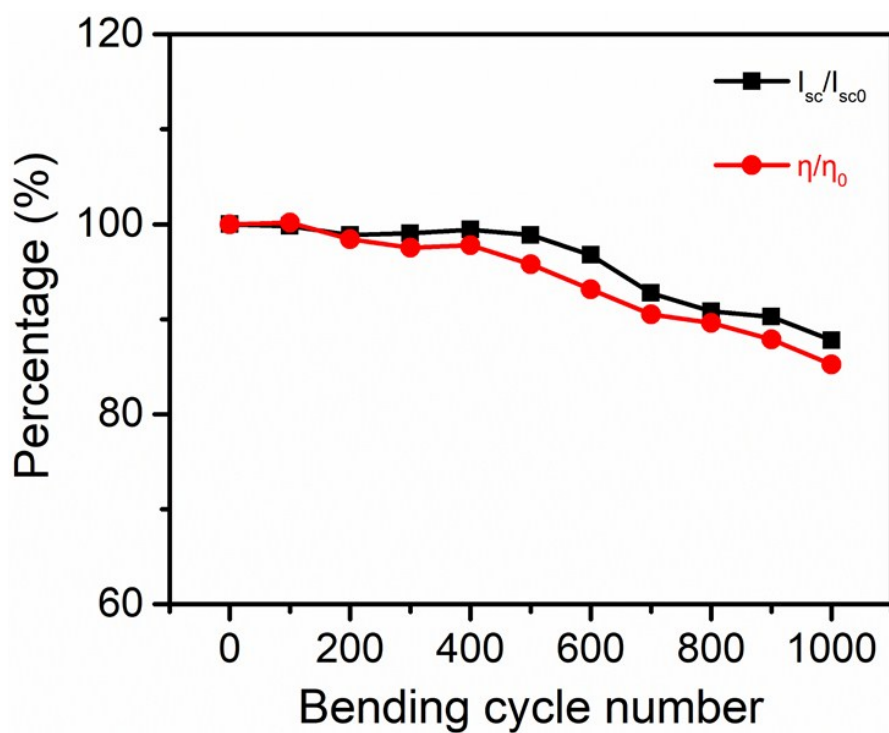


Figure S14. Dependence of photocurrent and PCE on bending cycle number for the PC part. I_{sc0} and I_{sc} correspond to the photocurrents before and after deformation, respectively. η_0 and η denoted the PCEs of the textile before and after deformation, respectively.

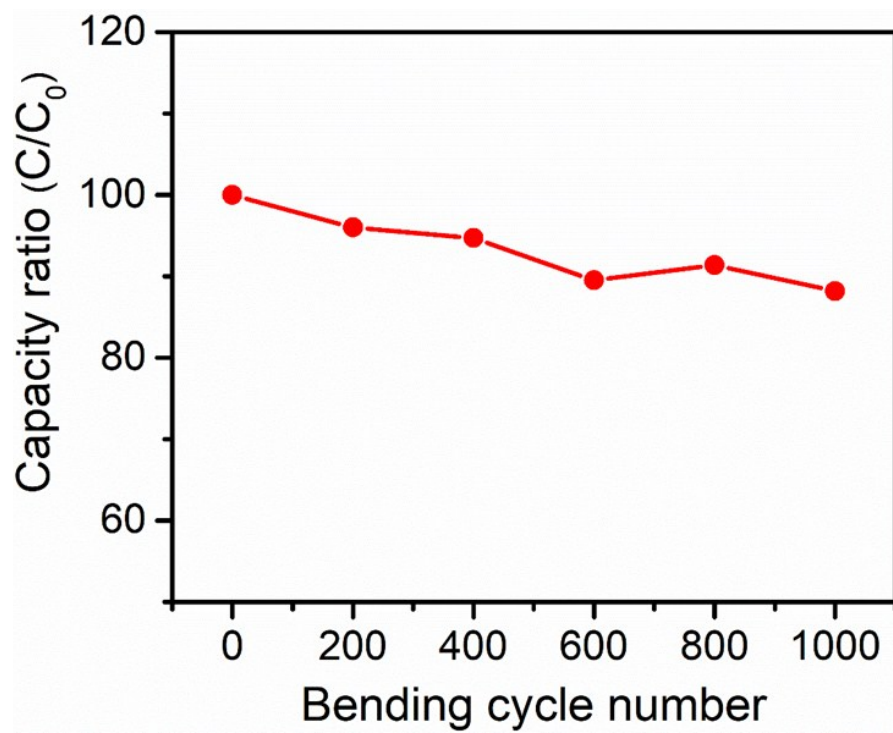


Figure S15. Dependence of capacity on bending cycle number for the ES part.

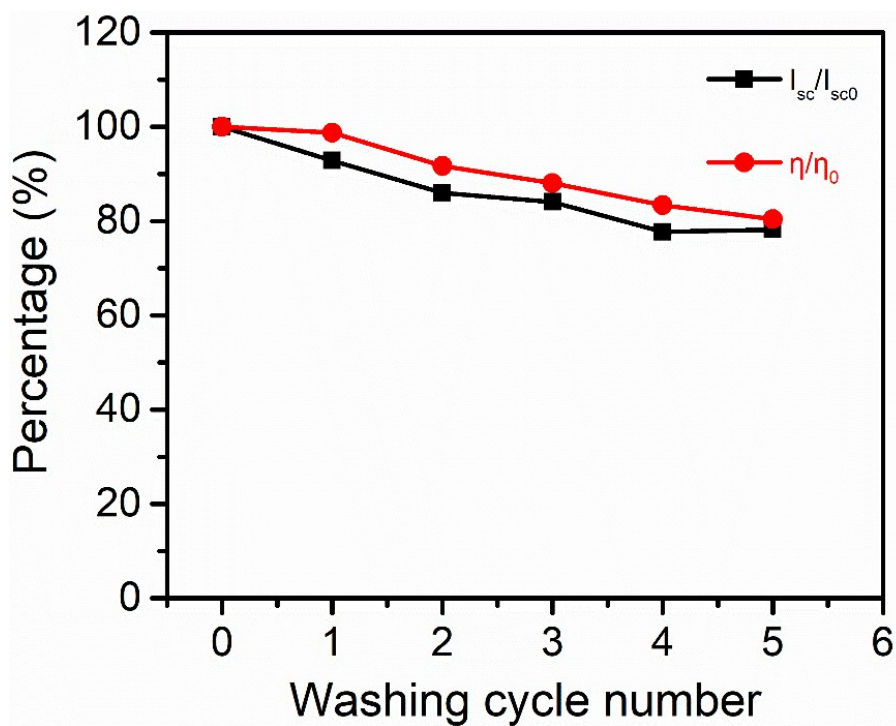


Figure S16. Dependence of photocurrent and PCE on washing cycle number for the PC part. I_{sc0} and I_{sc} correspond to the photocurrents before and after washing, respectively. η_0 and η denoted the PCEs of the textile before and after washing, respectively.

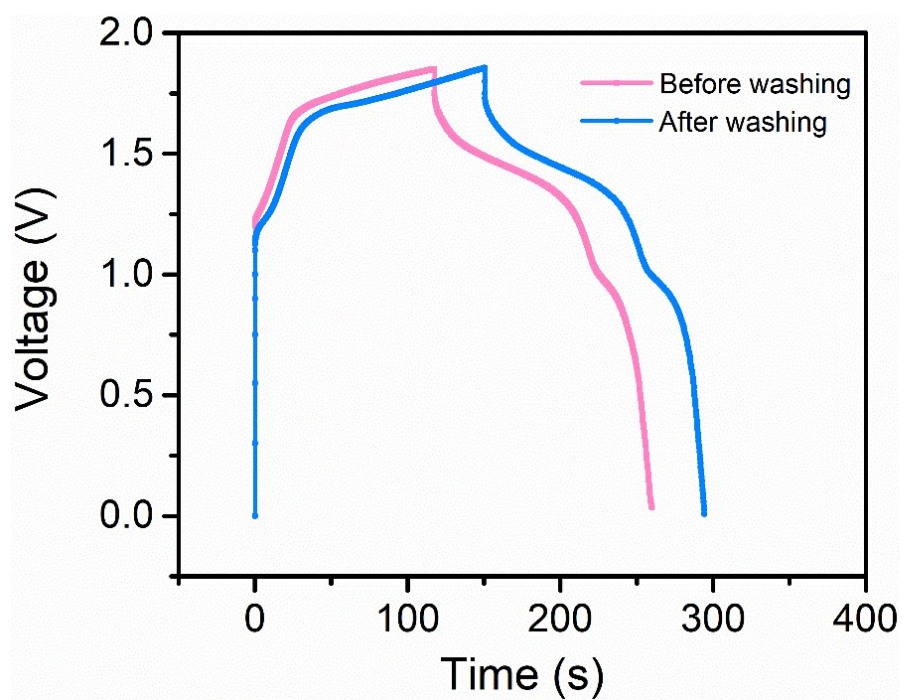


Figure S17. Photocharging and discharging curves before and after washing.

Table S1. Flexible self-powering textile compared with the other self-powered fiber devices reported in literature ^{a, 1-6}

EH part	ES part	Device structures	External circuit	Weaved by industrial loom	Size	Ref.
DSSCs/NGs	SCs	In-series	Need	No	~ 2 cm	1
DSSCs	SCs	In-series	Need	No	~ 4 cm	2
DSSCs	SCs	coaxial	Need	No	~ 4 cm	3
NGs	SCs	-	Need	No	~ 1.5 cm	4
DSSCs	LIBs	coaxial	Need	No	~ 6 cm	5
DSSCs	SCs/ LIBs	In-series	Need	No	~ 10 cm	6
ss-DSSCs	LIB	Interlaced	Needless	Yes	21 × 27 cm²	-

^{a)} DSSCs is dye-sensitized solar cells, ss-DSSC is solid-state dye-sensitized solar cells, NGs is nano generators, SCs is supercapacitors, and LIBs is Li-ion batteries

Table S2. Photovoltaic parameters of the PC part compared with the other reports.⁷⁻¹¹

Year	<i>V</i>_{oc} (V)	<i>J</i>_{sc} (mA/cm²)	FF (%)	PCE (%)	Ref.
2008	0.30	0.53	26.50	0.04	7
2011	0.36	6.49	58.00	1.38	8
2014	0.40	2.75	51.80	0.57	9
2015	0.45	3.8	47.83	0.82	10
2016	0.46	7.80	36.23	1.30	11
This work	0.40	9.42	51.45	1.92	-

Table S3. Photovoltaic parameters of the of the PC part woven from Ag-plated nylon yarns with different intervals under the illumination of AM 1.5 G, 100 mW/cm² ^a.

Interval (mm)	<i>V</i>_{oc} (V)	<i>J</i>_{sc} (mA/cm²)	FF (%)	PCE (Avg.) (%)
0.5	0.38	5.98	48.98	1.12 (1.04)
1.0	0.42	8.42	47.56	1.69 (1.51)
1.5	0.40	7.82	42.77	1.33(1.23)
2.0	0.38	6.13	42.08	0.98 (0.87)
2.5	0.37	5.30	38.06	0.75 (0.62)

^a) The average values were calculated over five devices.

References for the Supporting Information

- 1 J. Bae, Y. J. Park, M. Lee, S. N. Cha, Y. J. Choi, C. S. Lee, J. M. Kim, Z. L. Wang, *Adv. Mater.* 2011, **23**, 3446-3449.
- 2 X. Chen, H. Sun, Z. Yang, G. Guan, Z. Zhang, L. Qiu, H. Peng, *J. Mater. Chem. A* 2014, **2**, 1897-1902.
- 3 Z. Yang, J. Deng, H. Sun, J. Ren, S. Pan, H. Peng, *Adv. Mater.* 2014, **26**, 7038-7042.
- 4 J. Wang, X. Li, Y. Zi, S. Wang, Z. Li, L. Zheng, F. Yi, S. Li, Z. L. Wang, *Adv. Mater.* 2015, **27**, 4830-4836.
- 5 H. Sun, Y. Jiang, S. Xie, Y. Zhang, J. Ren, A. Ali, S.-G. Doo, I. H. Son, X. Huang, H. Peng, *J. Mater. Chem. A* 2016, **4**, 7601-7605.
- 6 J. Liang, G. Zhu, C. Wang, Y. Wang, H. Zhu, Y. Hu, H. Lv, R. Chen, L. Ma, T. Chen, *Adv. Energy Mater.* 2017, **7**, 1601208.
- 7 X. Fan, Z. Chu, L. Chen, C. Zhang, F. Wang, Y. Tang, J. Sun, D. Zou, *Appl. Phys. Lett.* 2008, **92**, 113510.
- 8 D. Wang, S. Hou, H. Wu, C. Zhang, Z. Chu, D. Zou, *J. Mater. Chem.* 2011, **21**, 6383-6388.
- 9 H. Feng, S. Tao, X. Zhang, J. Li, Z. Liu, X. Fan, *Chem. Commun.* 2014, **50**, 3509-3511.
- 10 X. Fan, X. Zhang, N. Zhang, L. Cheng, J. Du, C. Tao, *Electrochim. Acta* 2015, **161**, 358-363.
- 11 N. Zhang, J. Chen, Y. Huang, W. Guo, J. Yang, J. Du, X. Fan, C. Tao, *Adv. Mater.* 2016, **28**, 263-269.